Li-ion battery materials: present and future

Naoki Nitta[1,3], Feixiang Wu[1,2,3], Jung Tae Lee[1,3] and Gleb Yushin[1,*]

[1] School of Materials Science and Engineering, Georgia Institute of Technology, Atlanta, GA 30332, USA
[2] School of Metallurgy and Environment, Central South University, Changsha 410083, PR China

This review covers key technological developments and scientific challenges for a broad range of Li-ion battery electrodes. Periodic table and potential/capacity plots are used to compare many families of suitable materials. Performance characteristics, current limitations, and recent breakthroughs in the development of commercial intercalation materials such as lithium cobalt oxide (LCO), lithium nickel cobalt manganese oxide (NCM), lithium nickel cobalt aluminum oxide (NCA), lithium iron phosphate (LFP), lithium titanium oxide (LTO) and others are contrasted with that of conversion materials, such as alloying anodes (Si, Ge, Sn, etc.), chalcogenides (S, Se, Te), and metal halides (F, Cl, Br, I). New polyanion cathode materials are also discussed. The cost, abundance, safety, Li and electron transport, volumetric expansion, material dissolution, and surface reactions for each type of electrode materials are described. Both general and specific strategies to overcome the current challenges are covered and categorized.

Introduction

Li-ion batteries have an unmatchable combination of high energy and power density, making it the technology of choice for portable electronics, power tools, and hybrid/full electric vehicles [1]. If electric vehicles (EVs) replace the majority of gasoline powered transportation, Li-ion batteries will significantly reduce greenhouse gas emissions [2]. The high energy efficiency of Li-ion batteries may also allow their use in various electric grid applications, including improving the quality of energy harvested from wind, solar, geo-thermal and other renewable sources, thus contributing to their more widespread use and building an energy-sustainable economy. Therefore Li-ion batteries are of intense interest from both industry and government funding agencies, and research in this field has abounded in recent years.

Yet looking to the future, there are many who doubt that Li-ion batteries will be able to power the world's needs for portable energy storage in the long run. For some applications (such as transportation and grid) Li-ion batteries are costly at present, and a shortage of Li and some of the transition metals currently used in Li-ion batteries may one day become an issue [3]. At the same time, Li-ion batteries have certain fundamental advantages over other chemistries. Firstly, Li has the lowest reduction potential of any element, allowing Li based batteries to have the highest possible cell potential. Also, Li is the third lightest element and has one of the smallest ionic radii of any single charged ion. These factors allow Li-based batteries to have high gravimetric and volumetric capacity and power density. Finally, although multivalent cations allow for higher charge capacity per ion, the additional charge significantly reduces their mobility. Given that ionic diffusion in the solid electrodes is often the rate-limiting factor for battery power performance, this presents an enormous hurdle for the development of such alternative chemistries.

A significant shortage of Li is unlikely in the near future [4,5]. Similar claims have been made about peak oil, but have yet to materialize as world oil reserves and resources continue to grow with rising prices and the development of exploration and mining technologies. In terms of absolute quantities, the amount of Li available on the Earth's crust is sufficient to power a global fleet of automobiles [6]. Rising prices though, can be problematic for Li-ion batteries because cost is the major factor inhibiting its expansion into renewable energy applications. Even so, Li is not a major factor in the cost of Li-ion batteries at present. Li is used in the

*Corresponding author:. Yushin, G. (yushin@gatech.edu)
[3] These authors contributed equally to this study.

(a) Availability
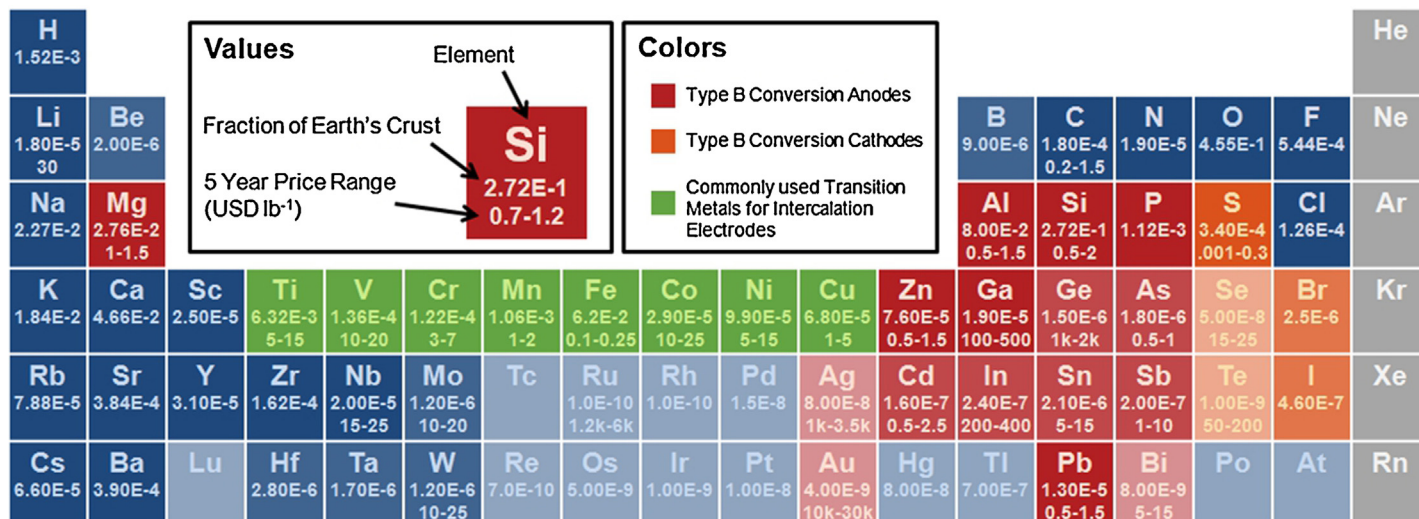
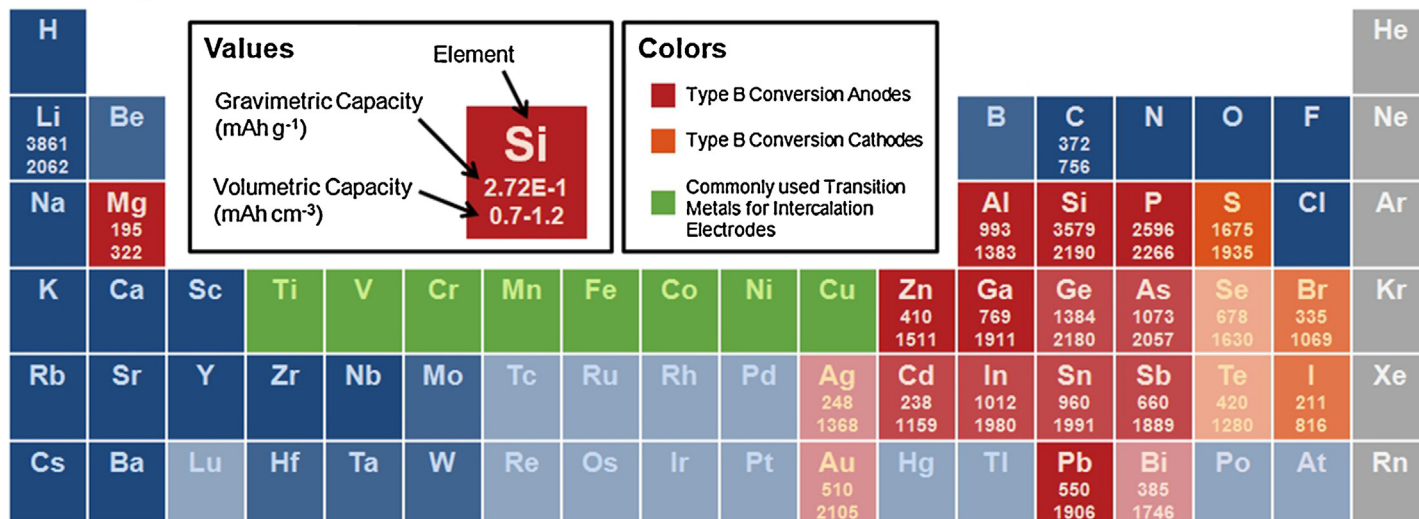

(b) Charge Capacity

FIGURE 1

(a) Availability and (b) capacities of elements that may host Li as electrodes. Elements with abundance (as fraction of Earth's crust) below 10^{-5} are slightly faded, and elements below 10^{-7} are faded further. Prices are approximate 5-year ranges of metal prices (except Ge, which is a 3 year range) [10–13], 80–100 mesh natural graphite for carbon [14], and the Vancouver/USGS prices for sulfur [13,15]. Gravimetric and volumetric capacities are theoretical values calculated based on delithiated mass and lithiated volume.

cathode and electrolyte, which make up only a small portion of the overall cost [7]. Within these components the cost of processing and the cost of cobalt in cathodes are the major contributing factors [8]. Given its fundamental advantages, Li-ion batteries will in all likelihood continue to dominate portable electrochemical energy storage for many years to come.

Since Li-ion batteries are the first choice source of portable electrochemical energy storage, improving their cost and performance can greatly expand their applications and enable new technologies which depend on energy storage. A great volume of research in Li-ion batteries has thus far been in electrode materials. Electrodes with higher rate capability, higher charge capacity, and (for cathodes) sufficiently high voltage can improve

the energy and power densities of Li batteries and make them smaller and cheaper. However, this is only true assuming that the material itself is not too expensive or rare.

Figure 1a shows the wholesale price of various metals and the abundance of elements as a fraction of the Earth's crust [9]. Although the electrodes are not fabricated from pure metal ingots, the prices illustrate the relative differences. Mn is clearly much cheaper than Co, explaining the cost difference in the cathode materials made from these two metals. The abundance of elements represents a limitation on the availability of the element. While true availability also depends on supply and demand, this chart shows advantages of some elements. For example, P and S are much more abundant than the more conductive elements in
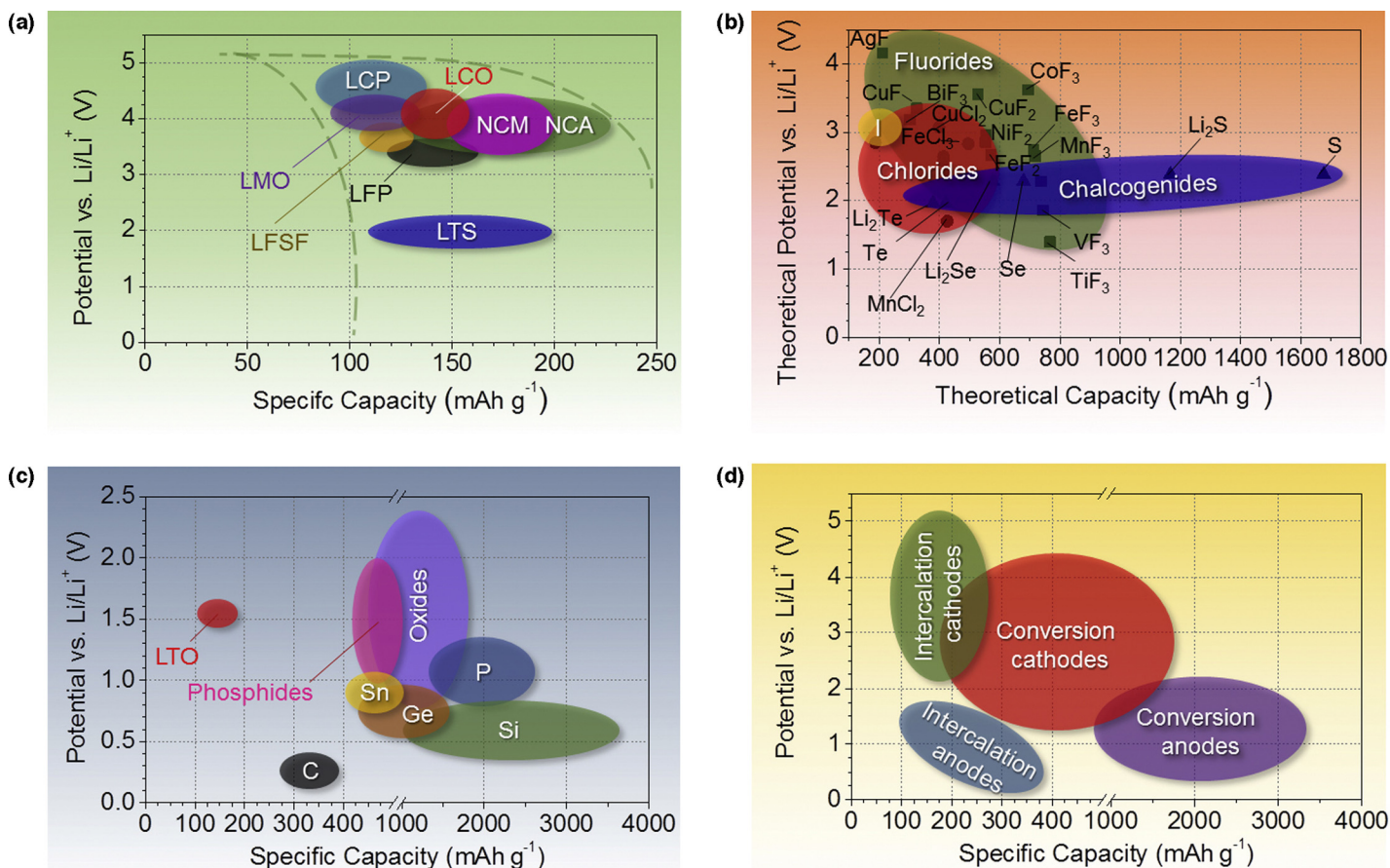
FIGURE 2

Approximate range of average discharge potentials and specific capacity of some of the most common (a) intercalation-type cathodes (experimental), (b) conversion-type cathodes (theoretical), (c) conversion type anodes (experimental), and (d) an overview of the average discharge potentials and specific capacities for all types of electrodes.

Groups V and VI, respectively. Finally, the theoretical specific and volumetric capacities of the elements which undergo conversion reactions with Li are shown in Fig. 1b.

Unfortunately, as useful as the periodic table is, most cathode materials are compounds, and are not suited for such a chart. Figure 2 is a fairly comprehensive form of a popular chart, depicting average electrode potential against experimentally accessible (for anodes and intercalation cathodes) or theoretical (for conversion cathodes) capacity. This allows the reader to evaluate various anode and cathode combinations and their theoretical cell voltage, capacity, and energy density. The chart can also be used to identify suitable electrolytes, additives, and current collectors for the electrode materials of choice. The acronyms for the intercalation materials (Fig. 2a) are: LCO for ''lithium cobalt oxide'', LMO for ''lithium manganese oxide'', NCM for ''nickel cobalt manganese oxide'', NCA for ''nickel cobalt aluminum oxide'', LCP for ''lithium cobalt phosphate'', LFP for ''lithium iron phosphate'', LFSF for ''lithium iron fluorosulfate'', and LTS for ''lithium titanium sulfide''.

To enable the application of new types of electrode materials, various strategies have been used. These strategies are summarized in Fig. 3, and are often similar regardless of type of material, crystal structure, or operating mechanism. In this review we will discuss a range of the representative cathode and anode materials, starting

from commercially available and currently used materials to promising novel materials that may be commercialized in the future. Fundamental properties, opportunities, challenges, and latest progress of anode and cathode material research will be discussed. It should be noted that although flexible batteries have recently been of high interest, we will not cover this topic in this review, and instead refer to other literature [16–21].

Cathodes
Intercalation cathode materials
An intercalation cathode is a solid host network, which can store guest ions. The guest ions can be inserted into and be removed from the host network reversibly. In a Li-ion battery, Li^+ is the guest ion and the host network compounds are metal chalcogenides, transition metal oxides, and polyanion compounds. These intercalation compounds can be divided into several crystal structures, such as layered, spinel, olivine, and tavorite (Fig. 4). The layered structure is the earliest form of intercalation compounds for the cathode materials in Li-ion batteries. Metal chalcogenides including TiS_3 and $NbSe_3$ were studied long ago as a possible intercalating cathode materials [24]. While TiS_3 exhibited only partial reversibility due to irreversible structure change from trigonal prismatic to octahedral coordination on lithiation, $NbSe_3$ demonstrated reversible electrochemical behavior. Among many
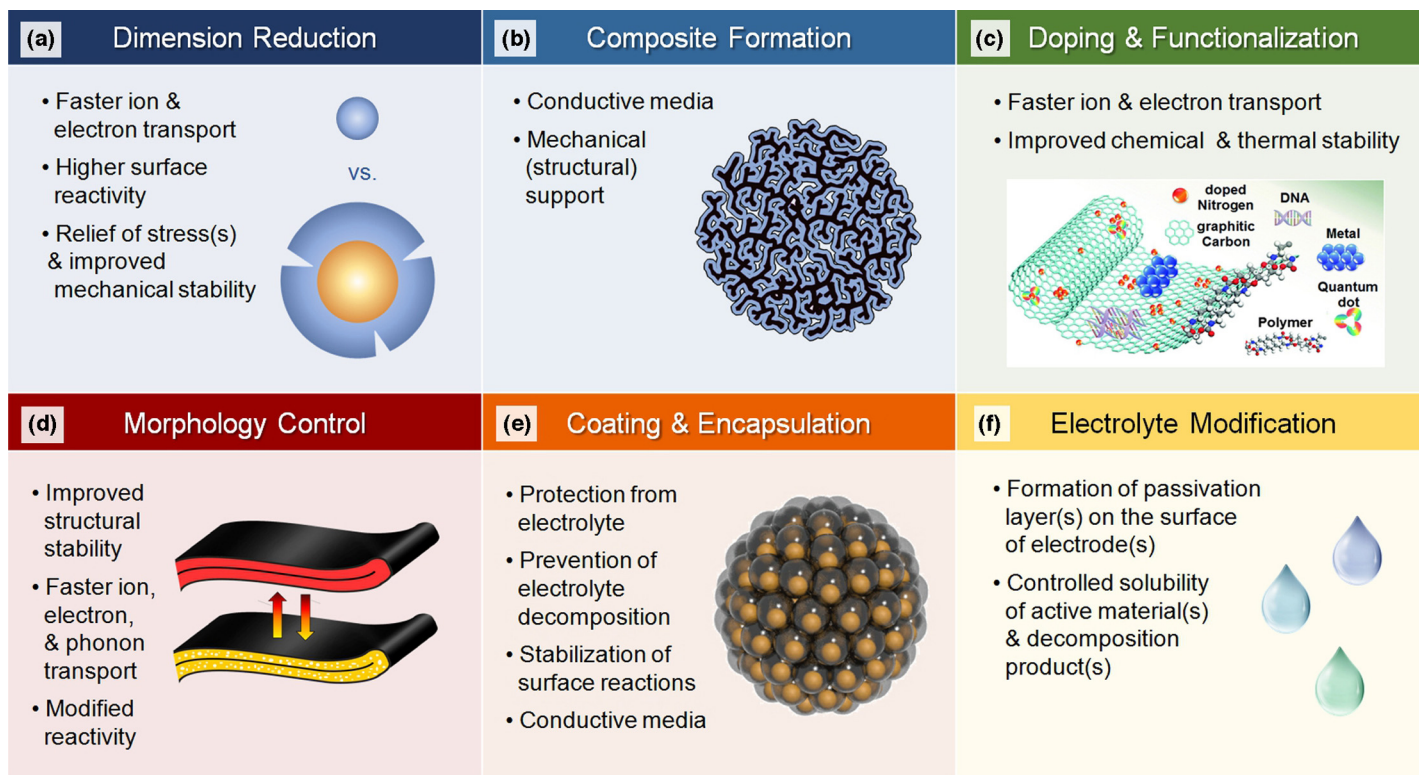
FIGURE 3

General strategies for performance enhancement and their rationale: (a) reducing dimensions of active materials, (b) formation of composites, (c) doping and functionalization, (d) tuning particle morphology, (e) formation of coatings or shells around active materials, (f) modification of electrolyte. Schematic figure in (c) reproduced with permission Copyright (2014) from The Royal Society of Chemistry [22], while schematic figure in (e) is reproduced with permission Copyright (2014) from Nature Publishing Group [23].

different types of chalcogenides, LiTiS$_2$ (LTS) was widely studied due to its high gravimetric energy density combined with long cycle life (1000+ cycles) and was eventually commercialized by Exxon [25,26]. However, most current intercalation cathode research is focused on the transition metal oxide and polyanion compounds due to their higher operating voltage and the resulting higher energy storage capability. Typically, intercalation cathodes have 100–200 mAh/g specific capacity and 3–5 V average voltage vs. Li/Li$^+$ (Fig. 4e, Table 1).

Transition metal oxide

LiCoO$_2$ (LCO) introduced by Goodenough [46] is the first and the most commercially successful form of layered transition metal oxide cathodes. It was originally commercialized by SONY, and this material is still used in the majority of commercial Li-ion batteries. The Co and Li, located in octahedral sites occupy alternating layers and form a hexagonal symmetry (Fig. 4a). LCO is a very attractive cathode material because of its relatively high theoretical specific capacity of 274 mAh g^{-1}, high theoretical volumetric capacity of 1363 mAh cm^{-3}, low self-discharge, high discharge voltage, and good cycling performance [47,48].

The major limitations are high cost, low thermal stability, and fast capacity fade at high current rates or during deep cycling. LCO cathodes are expensive because of the high cost of Co (Fig. 1). Low thermal stability refers to exothermic release of oxygen when a lithium metal oxide cathode is heated above a certain point, resulting in a runaway reaction in which the cell can burst into

flames [49]. Thermal runaway is a major concern in the application of Li-ion batteries, resulting, for example, in the grounding of all Boeing 787 airplanes in 2013 [50]. While this issue is general to transition metal oxide intercalation cathodes, LCO has the lowest thermal stability of any commercial cathode material [51]. Although thermal stability is also largely dependent on non-materials factors such as cell design and cell size, LCO typically experiences thermal runaway past ~200°C due to an exothermic reaction between the released oxygen and organic materials. Deep cycling (delithiation above 4.2 V, meaning approximately 50% or more Li extraction) induces lattice distortion from hexagonal to monoclinic symmetry and this change deteriorates cycling performance [52]. Many different types of metals (Mn, Al, Fe, Cr) [53–56] were studied as dopants/partial substitutes for Co and demonstrated promising but limited performance. Coatings of various metal oxides (Al$_2$O$_3$, B$_2$O$_3$, TiO$_2$, ZrO$_2$) [57,58] were more effective in enhancing LCO stability and performance characteristics even during deep cycling, because mechanically and chemically stable oxide material could reduce structural change of LCO and side reactions with electrolyte.

LiNiO$_2$ (LNO) has same crystal structure with LiCoO$_2$ and a similar theoretical specific capacity of 275 mAh g^{-1}. Its relatively high energy density and lower cost compared to Co based materials are the main research driving forces. However, pure LNO cathodes are not favorable because the Ni^{2+} ions have a tendency to substitute Li$^+$ sites during synthesis and delithiation, blocking the Li diffusion pathways [59]. LNO is also even more thermally
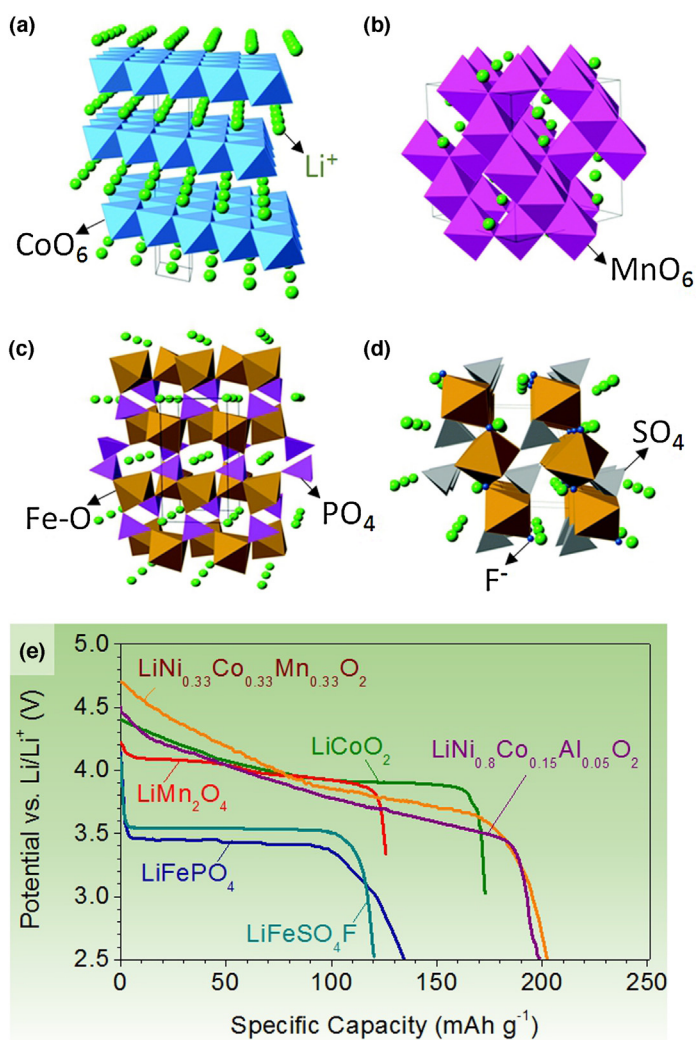
FIGURE 4

Crystal structures and discharge profiles of representative intercalation cathodes: structure of (a) layered (LiCoO$_2$), (b) spinel (LiMn$_2$O$_4$), (c) olivine (LiFePO$_4$), and (d) tavorite (LiFeSO$_4$F) (reproduced with permission Copyright (2014) Royal Society of Chemistry.) and (e) typical discharge profiles of intercalation cathodes [27–33].

unstable than LCO because Ni^{3+} is more readily reduced than Co^{3+} [60]. Partial substitution of Ni with Co was found to be an effective way to reduce cationic disorder [61]. Insufficient thermal stability at high state-of-charge (SOC) can be improved via Mg doping [62], and adding a small amount of Al can improve both thermal stability and electrochemical performance [63].

As a result, the LiNi$_{0.8}$Co$_{0.15}$Al$_{0.05}$O$_2$ (NCA) cathode has found relatively widespread commercial use, for example, in Panasonic batteries for Tesla EVs. NCA has high usable discharge capacity (~200 mAh g^{-1}) and long storage calendar life compared to conventional Co-based oxide cathode. However it was reported that capacity fade may be severe at elevated temperature (40–70°C) due to solid electrolyte interface (SEI) growth and micro-crack growth at grain boundaries [64,65].

LiMnO$_2$ (LMO) can also be promising because Mn is much cheaper and less toxic compare to Co or Ni. Anhydrous and stoichiometric layered LMO was prepared almost two decades ago [66], improving on a previous aqueous methods which in-duced impurities, different stoichiometries, poor crystallinity, and

undesirable structure change during cycling [67]. However, the cycling performance of LMO was still not satisfactory (i) because the layered structure has a tendency to change into spinel structure during Li ion extraction [67] and (ii) because Mn leaches out of LMO during cycling [31]. Mn dissolution occurs when Mn^{3+} ions undergo a disproportionation reaction to form Mn^{2+} and Mn^{4+}, and this process is observed for all cathodes containing Mn. Mn^{2+} is thought to be soluble in the electrolyte, and destabilize the anode SEI. Indeed, Mn concentration in the electrolyte and anode SEI has been observed to increase with aging for Mn containing cathodes [68–71]. Also, the anode impedance is seen to increase with Mn dissolution on carbon anodes [70], but not LTO [72] (which has a negligible SEI). Stabilization of LMO via cationic doping was conducted both experimentally and theoretically [73,74], but even so, the poor cycle stability of LMO (especially at elevated temperatures) has hindered widespread commerciali-zation.

Continuous research efforts on developing cathode material less expensive than LCO resulted in the formulation of the Li(Ni$_{0.5}$Mn$_{0.5}$)O$_2$ (NMO) cathode. NMO could be an attractive material because it can maintain similar energy density to LCO, while reducing cost by using lower cost transition metals. The presence of Ni allows higher Li extraction capacity to be achieved. However, cation mixing can cause low Li diffusivity and may result in unappealing rate capability [75]. Recent ab initio computational modeling predicted that low valence transition metal cations (Ni^{2+}) provides high-rate pathways and low strain, which are the crucial factors to achieve high rate capability in layered cathodes. NMO recently synthesized by ion exchange method showed a very low concentration of defects in NMO and capacity as high as ~180 mAh g^{-1} even at a very high rate of 6 C [76].

Adding Co into Li(Ni$_{0.5}$Mn$_{0.5}$)O$_2$ was found to be effective way to enhance the structure stability further [77]. LiNi$_x$Co$_y$Mn$_z$O$_2$ (NCM, aka NMC) has similar or higher achievable specific capacity than LCO and similar operating voltage while having lower cost since the Co content is reduced. LiNi$_{0.33}$Co$_{0.33}$Mn$_{0.33}$O$_2$ is the common form of NMC and is widely used in the battery market. Some of the recent efforts, such as formation of macroporous NMC, showed reversible specific capacity as high as 234 mAh g^{-1} 1 and good cycle stability even at 50°C [78]. Li$_2$MnO$_3$ stabilized LiMO$_2$ (where M = Mn, Ni, Co) can also achieve high capacity (>200 mAh g^{-1}) under high voltage operation (4.5–3.0 V) [79]. Li$_2$MnO$_3$ is activated at >4.5 V, releasing Li$_2$O [80] on the initial cycle which provides extra Li$^+$. The remaining Li$_2$MnO$_3$ can also facilitate Li diffusion and also act as a Li reservoir. This material group is called a lithium-rich layered oxide compound due to its extra Li ion compared to the common layered structure. More recently, novel cathode material with average composition of LiNi$_{0.68}$Co$_{0.18}$Mn$_{0.18}$O$_2$, in which each particle consists of bulk material surrounded by a concentration-gradient outer layer was reported [81]. The bulk material is a nickel-rich layered oxide (LiNi$_{0.8}$Co$_{0.1}$Mn$_{0.1}$O$_2$) for higher energy/power density (higher Ni content allows for higher Li extraction without structure deterioration), while the outer layer is Mn and Co substituted NMC (LiNi$_{0.46}$Co$_{0.23}$Mn$_{0.31}$O$_2$) for better cycle life and safety. It is proposed that the stability of this material could originate from stable Mn^{4+} in the surface layer, hence the gas evolution due to reaction between Ni ion and electrolyte is delayed.

TABLE 1

Characteristics of representative intercalation cathode compounds; crystal structure, theoretical/experimental/commercial gravimetric and volumetric capacities, average potentials, and level of development.

Crystal structure	Compound	Specific capacity (mAh g^{-1}) (theoretical/experimental/typical in commercial cells)	Volumetric capacity (mAh cm^{-3}) (theoretical/ typical in commercial cells)	Average voltage (V) [34]	Level of development
Layered	LiTiS$_2$	225/210 [35]	697	1.9	Commercialized
	LiCoO$_2$	274/148 [36]/145	1363/550	3.8	Commercialized
	LiNiO$_2$	275/150 [37]	1280	3.8	Research
	LiMnO$_2$	285/140 [38]	1148	3.3	Research
	LiNi$_{0.33}$Mn$_{0.33}$Co$_{0.33}$O$_2$	280/160 [32]/170	1333/600	3.7	Commercialized
	LiNi$_{0.8}$Co$_{0.15}$Al$_{0.05}$O$_2$	279/199 [33]/200	1284/700	3.7	Commercialized
	Li$_2$MnO$_3$	458/180 [39]	1708	3.8	Research
Spinel	LiMn$_2$O$_4$	148/120 [40]	596	4.1	Commercialized
	LiCo$_2$O$_4$	142/84 [41]	704	4.0	Research
Olivine	LiFePO$_4$	170/165 [42]	589	3.4	Commercialized
	LiMnPO$_4$	171/168 [43]	567	3.8	Research
	LiCoPO$_4$	167/125 [44]	510	4.2	Research
Tavorite	LiFeSO$_4$F	151/120 [30]	487	3.7	Research
	LiVPO$_4$F	156/129 [45]	484	4.2	Research

Spinel Li$_2$Mn$_2$O$_4$ (also LMO) [82] benefits from the abundance, cost, and environmental friendliness of Mn. Li occupies tetrahedral 8a sites and Mn is located in octahedral 16d sites in a ccp array of oxygen anions (Fig. 4b). Li$^+$ can diffuse through vacant tetrahedral and octahedral interstitial sites in the three-dimensional structure. The insufficient long-term cyclability is believed to originate from irreversible side reactions with electrolyte, oxygen loss from the delithiated LiMn$_2$O$_4$, Mn dissolution, and formation of tetragonal Li$_2$Mn$_2$O$_4$ at the surface especially at the fast c-rates [83,84]. By using nanoparticles, the rate performance can be greatly improved due to shorter Li$^+$ diffusion lengths and improved electronic transport. Many different groups have synthesized LMO nanowires and mesoporous LMO, which show promising results [85–89]. Although decreased diffusion lengths also exacerbates the dissolution problem, it can be repressed with a surface coating of ZnO [90], Mn-rich layered structure [40], metal doping [91], oxygen stoichiometry [92], blending with different cathode materials [93], and forming a stable cathode SEI layer [94,95]. Recently, a novel ordered mesoporous lithium rich Li$_{1.12}$Mn$_{1.88}$O$_4$ spinel was demonstrated to improved electrochemical performance compare to bulk spinel [96].

Polyanion compounds

In exploring new cathode materials, researchers have developed a new class of compounds called polyanions. Large $(XO_4)^{3-}$ (X = S, P, Si, As, Mo, W) polyanions occupy lattice positions and increase cathode redox potential while also stabilizing its structure [97]. LiFePO$_4$ (LFP) is the representative material for the olivine structure, known for its thermal stability [51] and high power capability. In LFP, Li$^+$ and Fe^{2+} occupy octahedral sites, while P is located in tetrahedral sites in a slightly distorted hexagonal close-packed (HCP) oxygen array (Fig. 4c). The major weaknesses of the LiFePO$_4$ cathode include its relatively low average potential (Fig. 4e, Table 1) and low electrical and ionic conductivity. Intensive research over the last decade resulted in significant improvements in both performance and mechanistic understanding of LFP. Reduction in particle size in combination with carbon coating [98] and cationic

doping [99] were found to be effective in increasing the rate performance. It is noteworthy that good electrochemical performance can also be achieved without carbon coating if particles are uniformly nano-sized and conductive nanocarbons are used within the cathodes [100]. Virus-templated amorphous anhydrous FP/CNT composite, for example, demonstrated promising results [101]. It was reported that the facile redox reaction in non-conducting LFP could be due to a curved one-dimensional lithium diffusion path through the [0 1 0] direction [102]. In general, however, the low density of nanostructured LFP electrodes and their low average potential limit the energy density of LFP cells. Recently, a novel non-olivine allaudite LFP was reported and showed fundamentally different electrochemical behavior from that of olivine LFP [103].
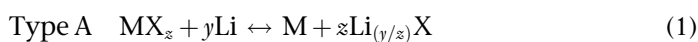
Other olivine structures include LiMnPO$_4$ (LMP) which offers ∼0.4 V higher average voltage compared to olivine LFP (Table 1), leading to higher specific energy, but at the expense of lower conductivity [104]. LiCoPO$_4$, LiNi$_{0.5}$Co$_{0.5}$PO$_4$, and LiMn$_{0.33}$Fe$_{0.33}$Co$_{0.33}$PO$_4$ (LCP, NCP, MFCP) have also been developed and shown promising results, but further improvements in power, stability and energy density are required [105–107]. Novel Li$_3$V$_2$(PO$_4$)$_3$ (LVP) exhibited relatively high operating voltage (4.0 V) and good capacity (197 mAh/g) [108]. Quite remarkably, LVP/C nanocomposite exhibited 95% theoretical capacity at a high rate of 5 C in spite of the low electronic conductivity of LVP (similar with LFP).

LiFeSO$_4$F (LFSF) is yet another interesting cathode material because of its high cell voltage and reasonable specific capacity (151 mAh g^{-1}) [109]. Fortunately LiFeSO$_4$F has better ionic/electronic conductivity hence it does not desperately need carbon coating and/or nanoparticles. LiFeSO$_4$F can also be economical since it can be prepared with abundant resources. LiFeSO$_4$F is composed of two slightly distorted Fe^{2+}O$_4$F$_2$ oxyfluoride octahedra connected by F vertices in the trans position, forming chains along the c-axis, and the Li$^+$ are located along the (1 0 0), (0 1 0), and (1 0 1) directions (Fig. 4d). Tavorite-structured cathode materials were evaluated via simulation and reported that the fluorosulfate and fluorophosphate families of materials are the most promising,

and the oxysulfate family is the least [110]. The tavorite structured materials with 1D diffusion channels were suggested to exhibit low activation energies, allowing charge and discharge of Fe(SO$_4$)F and V(PO$_4$)F at very high rates, comparable to those observed in small olivine Fe(PO$_4$) particles. The vanadium-containing material, LiVPO$_4$F, cycles well, and has high voltage and capacity [45,111] but raise concerns about toxicity and environmental impact. Interestingly, Li$^+$ can be intercalated at ~1.8 V hence this material is able to be used in both anode (Li$_{1+x}$VPO$_4$ where x = 0–1) and cathode (Li$_{1-x}$VPO$_4$ where x = 0–1). For further detailed information on synthesis method, chemical properties and mechanism, much more specialized reviews are available elsewhere [112,113].

Conversion cathode materials

Conversion electrodes undergo a solid-state redox reaction during lithiation/delithiation, in which there is a change in the crystalline structure, accompanied by the breaking and recombining chemical bonds. The full reversible electrochemical reaction for conversion electrode materials is generally as follows:

$$\text{Type A} \quad MX_z + y\text{Li} \leftrightarrow M + z\text{Li}_{(y/z)}X \quad (1)$$

$$\text{Type B} \quad y\text{Li} + X \leftrightarrow \text{Li}_yX \quad (2)$$

For cathodes, the Type A category (Eq. (1)) includes metal halides comprising high (2 or more) valence metal ions to give higher theoretical capacities. Figure 5a [114] shows how this reaction takes place for FeF$_2$ particles. The F ions, having the
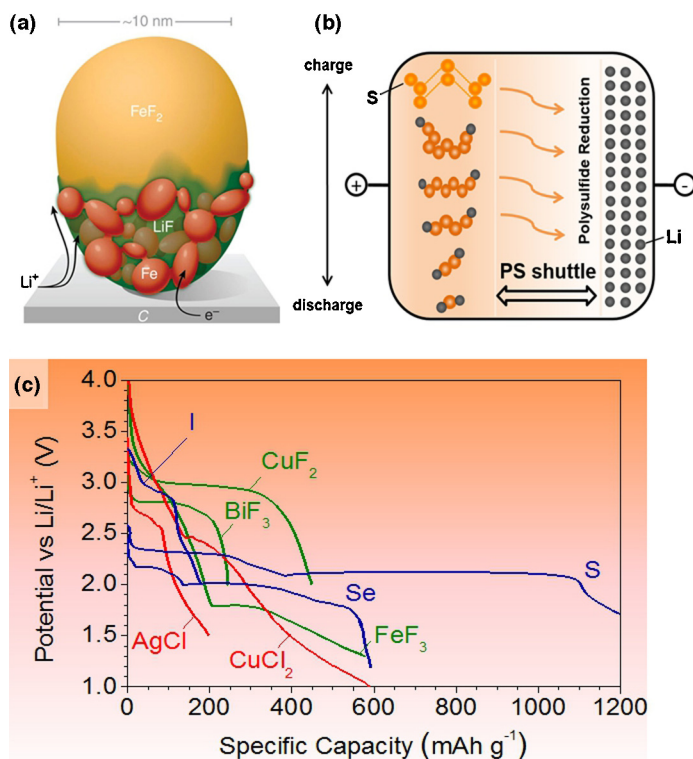

higher mobility, diffuse out of the FeF$_2$, and form LiF while nanosized phases of Fe form behind it [115]. This results in metal nanoparticles scattered in a 'sea' of the LiF (Li$_{(y/z)}$X from Eq. (1)). The same mechanism can be more or less observed for all Type A active materials, although an intermediate Li insertion phase can also form for some.

S, Se, Te, and I follow the Type B reaction (Eq. (2)). Of these elements, S has been studied the most because of its high theoretical specific capacity (1675 mAh g^{-1}), low cost, and abundance in the Earth's crust. Oxygen is also a Type B cathode in lithium air batteries, but poses fundamentally different technological hurdles because it is a gas. Attempts to use ambient air further complicate the issue at a systems level. Lithium air batteries are therefore not covered in this review.

Figure 5b shows the intermediate steps for the full S conversion reaction, which involves intermediate polysulfides soluble in organic electrolytes. Figure 5c shows the typical discharge curves of conversion cathodes. BiF$_3$ [116] and CuF$_2$ [117] show promising discharge profiles with high voltage plateaus. In comparison, Li$_2$S [118], S [119] and Se [120] also show very flat and long voltage plateaus, indicating good kinetics of the reaction between two solid phases.

Fluorine and chlorine compounds

Metal fluorides (MF) and chlorides (MCl) have recently been actively pursued due to intermediate operation voltages and high theoretical specific and volumetric capacities. However, MF and MCl generally suffer from poor conductivity, large voltage hysteresis, volume expansion, unwanted side reactions, and dissolution of active material (Table 2). Most MF, including FeF$_3$ and FeF$_2$, are notorious for their poor electronic conductivity because of the large band gap induced by the highly ionic character of the metal-halogen bond. However their open structures can support good ionic conduction [126,127]. Chlorides also suffer from poor electronic conductivity for the same reason. All of the reported MF and MCl materials show very high voltage hysteresis for reasons such as poor electronic conductivity and ion mobility (Table 2) [128].

Additionally, Type A conversion materials form metal nanoparticles at their fully lithiated state. BiF$_3$ and FeF$_2$ have been reported to catalyze the decomposition of cyclic carbonates at relatively high voltages, reducing cycle life [116,129]. On the other hand, Cu nanoparticles can be electrochemically converted to Cu^{1+}, which then dissolves into the electrolyte [130]. Even if such unwanted side reactions do not occur, metal nanoparticles may coalesce over the course of many cycles, exacerbating the voltage hysteresis [131].

Many ionic compounds are soluble in polar solvents, and this is true for some fluorides as well [135]. Metal chlorides (including LiCl) are even more susceptible to dissolution in various solvents, including those that are used in Li battery electrolytes [154]. Meanwhile, the volume expansions of MF and MCl, as calculated by using room temperature densities of compounds before and after lithiation [155], are somewhat moderate (Table 2). The most widely studied MF and MCl materials exhibit volume expansions of 2–25%. While not nearly as high as for Type B conversion cathode materials and conversion/alloying anode materials (to be discussed in the following sections), issues such as fracturing and loss of electrical contact are still possible.

FIGURE 5

Transformations accompanying selected conversion-type cathodes: (a) propagation of lithiation reaction front through a single FeF$_2$ particle [114] (reproduced with Permission Copyright (2014) from Nature Publishing Group); (b) polysulfides shuttle accompanying charge and discharge of a S particle and [121] and (c) typical discharge profiles of conversion cathodes [116,117,119,122–125].

TABLE 2

Challenges including conductivity, volume expansion, voltage hysteresis and cathode dissolution of conversion cathodes.

Materials	Electronic conductivity (S m^{-1})	Theoretical potential (V)	Volume expansion fraction (%)	Voltage hysteresis V (vs. Li)	Qualitative solubility in organic electrolytes
FeF$_2$	Insulator [132]	2.66	16.7	0.7–1 [115,132]	–
FeF$_3$	Insulator [126]	2.74	25.6	0.8–1.6 [124,126,133,134]	–
CoF$_2$	Poor [126]	2.85	21	0.8–1.2 [135]	Soluble [135]
CuF$_2$	Insulator [117,126,127]	3.55	11.6	0.8 [136]	–
NiF$_2$	Poor [126]	2.96	28.3	0.8–2 [137,138]	–
BiF$_3$	Poor [126]	3.18	1.76	0.5–0.7 [116,129]	–
FeCl$_3$	Poor	2.83	22.6	–	Soluble
FeCl$_2$	Poor	2.41	19.9	–	Soluble
CoCl$_2$	Poor	2.59	23	1 [139]	Soluble
NiCl$_2$	Poor	2.64	30.3	–	Soluble
CuCl$_2$	Poor	3.07	21.1	1.2 [123]	Soluble
AgCl	Poor	2.85	19.4	0.25 [123]	Insoluble [123]
LiCl	Poor	–	–	–	Soluble
S	Insulator 5 × 10^{-30} [140]	2.38	79	0.12–0.40 [119,140,141]	Soluble Intermediates
Li$_2$S	Insulator [142,143]	2.38	–	0.12–0.4 [144–147]	Soluble Intermediates
Se	Semiconductor 10^{-5} [148]	2.28	82.5	0.2–2.0 [120,125,149–152]	Soluble Intermediates
Li$_2$Se	Poor	2.28	–	–	Soluble Intermediates
Te	Semiconductor 2 × 10^2 [153]	1.96	104.7	0.3 [153]	–
I	Poor	3.01	49.3	0.2 [122]	Soluble [122]
LiI	Poor	3.01	–	–	Soluble [122]

In order to overcome their low conductivities, synthesis of nanoparticles of conversion materials is essential to shortening the pathway for the electrons and ions. For MF and MCl, active materials are often dispersed onto or wrapped in some conductive matrix materials to prepare composites with improved conductivity, such as FeF$_3$/CNT [156], FeF$_3$/graphene [157,158], AgCl/acetylene black [123] and BiF$_3$/MoS$_2$/CNT [129]. Electrolyte modifications are also important [116] to minimize unfavorable reactions between the electrolyte and active material during various stages of charge and discharge.

Sulfur and lithium sulfide

Sulfur has an extremely high theoretical capacity at 1675 mAh g^{-1}, while also being low cost and abundant in the Earth's crust. However, S based cathodes suffer from low potential vs. Li/Li$^+$, low electrical conductivity, dissolution of intermediate reaction products (polysulfides) in electrolyte, and (in the case of pure S) very low vaporization temperature, which induces S loss while drying the electrodes under vacuum. Sulfur also suffers from ~80% volume change [159], which may destroy the electrical contact in standard carbon composite electrodes [160]. To mitigate the effects of both dissolution and volume expansion, S can be encapsulated in a hollow structure with excess internal void space. Polyvinyl pyrrolidone polymer [161], carbon [162], and TiO$_2$ [163] capsules have been impregnated with sulfur by using infiltration and chemical precipitation. When tested in half cells in thin electrode configurations, these composites show cycle life sometimes approaching 1000 cycles.

To avoid the negative effects of expansion, prevent S evaporation during drying, and form full cells with Li free (and thus safer) anodes, electrodes have also been fabricated in the form of Li$_2$S [142,144,145,147,164–171]. Li$_2$S is not easily infiltrated into a host as with S because it has a much higher melting point. However, the high solubility of Li$_2$S in various environmentally friendly solvents (such as ethanol) can be utilized to form various Li$_2$S based

nanocomposites such as, for example, Li$_2$S nanoparticles embedded within a conductive carbon [144]. Because the fully lithiated Li$_2$S does not expand any further, no void spaces are necessary. In fact, carbon-coated Li$_2$S showed no change in morphology after 400 charge/discharge cycles [147].

Electrolyte modification is a popular method for mitigating polysulfide dissolution (Fig. 3f). LiNO$_3$ [172] and P$_2$S$_5$ [173] additives were used to form good SEI on the surface of Li metal to prevent the reduction and consequent precipitation of polysulfides. Lithium polysulfides can also be added to temporarily decrease cathode dissolution [174]. Multiple papers also utilized higher molarity electrolytes, which also greatly reduces polysulfide solubility [175,145,176]. Finally, solid state electrolytes can also prevent polysulfide dissolution, and at the same time, enhance cell safety by avoiding Li dendrite short circuiting [167,177–179].

Selenium and tellurium

Recently, Se and Te have attracted attention due to their higher electronic conductivities than S and high theoretical volumetric capacities of 1630 mAh cm^{-3} and 1280 mAh cm^{-3}, respectively, in the fully lithiated state. Due to the higher electronic conductivity, Se and Te often show higher utilization of active materials and higher rate capability than S. Similar to S, the Se-based cathodes suffer from the dissolution of high-order polyselenides [120], resulting in fast capacity loss, poor cycle performance and low coulombic efficiency. So far, the dissolution of polytelluride has not been reported. As seen in Table 2, elemental Se and Te also suffer from large volume change. Fortunately, Se and Te are also similar to S in that they have low melting points. Both materials have been infiltrated into various porous carbon hosts [120,153,180], and dispersed or wrapped in conductive matrices [125,149] to improve their performance. However, Te is far too expensive for practical use. Moreover, Se and Te are of similar abundance as Ag and Au (Fig. 1), and are very unlikely to be used in mass production.

Iodine

The lithium-iodine primary battery uses LiI as a solid electrolyte (10^{-9} S cm^{-1}), resulting in low self-discharge rate and high energy density, and is an important power source for implantable cardiac pacemaker applications. The cathodic I is first reduced into the tri-iodide ion (I_3^-) and then into the iodide ion (I^-) during discharge [122]. For use in most other applications, this chemistry is problematic, however, because of its low power capability. Furthermore, in standard organic electrolytes, iodine, triodide, and lithium iodide are all soluble [122]. Due to the high solubility of LiI in organic solvents, iodine ions have been considered for use in lithium-flow batteries instead. Recently, active iodine was infiltrated into the pores of porous carbon due to low melting point of I (113°C). The as-produced iodine–conductive carbon black composite showed a high discharge voltage plateau, good cycle performance, and high rate capability, which is attributed to the enhanced electronic conductivity and suppressed active material dissolution [122].

Anode

Anode materials are necessary in Li-ion batteries because Li metal forms dendrites which can cause short circuiting, start a thermal run-away reaction on the cathode, and cause the battery to catch fire. Furthermore, Li metal also suffers from poor cycle life. While the major efforts to enable Li metal anodes have been reviewed by others [181], this topic will not be covered herein. Instead, this section provides a concise overview of secondary anode materials. For further investigation, we recommend other more detailed reviews on carbon [182], lithium titanium oxide (LTO) [183,184], and Type A and Type B conversion anode materials [185–187].

Graphitic and hard carbons

The carbon anode enabled the Li-ion battery to become commercially viable more than 20 years ago, and still is the anode material of choice. Electrochemical activity in carbon comes from the intercalation of Li between the graphene planes, which offer good 2D mechanical stability, electrical conductivity, and Li transport (Fig. 6a). Up to 1 Li atom per 6 C can be stored in this way. Carbon has the combined properties of low cost, abundant availability, low delithiation potential vs Li, high Li diffusivity, high electrical conductivity, and relatively low volume change during lithiation/delithiation (Table 3). Thus carbon has an attractive balance of relatively low cost, abundance, moderate energy density, power density, and cycle life, compared to any other intercalation-type anode materials. Carbon's gravimetric capacity is higher than most cathode materials (Fig. 2), but the volumetric capacity of commercial graphite electrodes is still small (330–430 mAh cm^{-3}).
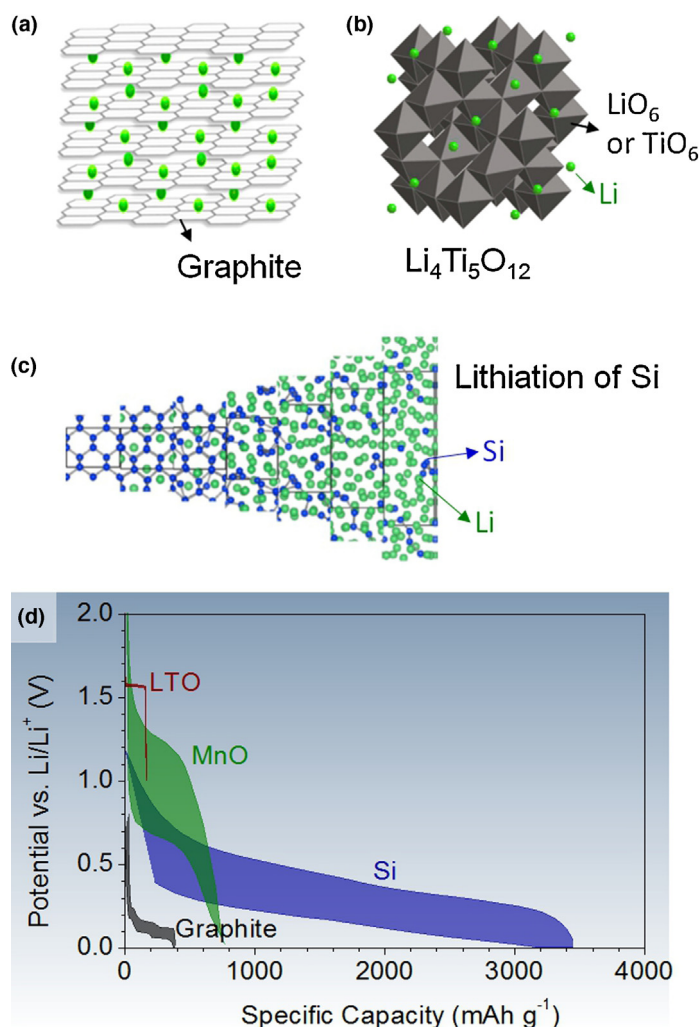
FIGURE 6

Crystal structures of (a) lithiated graphite [188], (b) lithium titanate (LTO) [189], and (c) silicon during lithiation [190] (reproduced with Permission Copyright (2014) American Chemical Society) and (d) charge–discharge profiles at low charge/discharge rates, showing voltage hysteresis [191–193].

Commercial carbon anodes can be largely divided into two types. Graphitic carbons have large graphite grains and can achieve close to theoretical charge capacity. However, graphitic carbons do not combine well with a propylene carbonate (PC)-based electrolyte, which is preferred due to a low melting point and fast Li transport. PC intercalates together with the Li$^+$ between the graphitic planes, causing the graphite to exfoliate and lose capacity [217]. Even without solvent intercalation, Li intercalation occurs at the basal planes, and thus the SEI also preferentially

TABLE 3

Properties of some commonly studied anode materials.

Material	Lithiation potential (V)	Delithiation potential (V)	D (cm^2 s^{-1})	Volume change
Graphite [182,193–198]	0.07, 0.10, 0.19	0.1, 0.14, 0.23	10^{-11}–10^{-7}	10%
LTO [199–203]	1.55	1.58	10^{-12}–10^{-11}	0.20%
Si [34,191,204–209]	0.05, 0.21	0.31, 0.47	10^{-13}–10^{-11}	270%
Ge [34,209–212]	0.2, 0.3, 0.5	0.5, 0.62	10^{-12}–10^{-10}	240%
Sn [34,209,213–215]	0.4, 0.57, 0.69	0.58, 0.7, 0.78	10^{-16}–10^{-13}	255%
Li$_2$O [216] **(amorphous)**	N/A	N/A	5×10^{-12}–5×10^{-10}	N/A

forms on these planes as well [218]. During Li intercalation, single crystalline graphitic particles undergo uniaxial 10% strain along the edge planes [197,198]. Such large strain may damage the SEI and reduce the cell's cycle life. Recently, graphitic carbons have been coated with a thin layer of amorphous carbon [219,220] to protect the vulnerable edge planes from electrolyte and achieve high coulombic efficiency.

Hard carbons have small graphitic grains with disordered orientation, and are much less susceptible to exfoliation. These grains also have nanovoids between them, resulting in reduced and isotropic volume expansion. Nanovoids and defects also provide excess gravimetric capacity, allowing capacity in excess of the theoretical 372 mAh g^{-1} [182,221–223]. Together, these properties make hard carbons a high capacity high cycle life material. However, the high fraction of exposed edge planes increases absolute quantity of SEI formed, reducing the coulombic efficiency in the first few cycles. Given that a full Li-ion cell has a limited Li inventory, this represents a serious disadvantage in terms of achievable capacity. Also, the void spaces significantly reduce the density of the particles, further decreasing volumetric capacity.

Finally, impurities such as hydrogen atoms can also provide extra capacity in carbon based anodes [224]. However, such electrodes suffer from larger voltage hysteresis, higher irreversible capacity loss, and even lower volumetric capacity, and thus are unlikely to be commercialized [223].

Lithium titanium oxide (Li$_4$Ti$_5$O$_{12}$/LTO)

LTO has been successfully commercialized because it allows the combination of superior thermal stability [51], high rate, relatively high volumetric capacity, and high cycle life, despite the higher cost of Ti, the reduced cell voltage, and lower capacity (175 mAh g^{-1} & 600 mAh cm^{-3} theoretical). High rate and stability originates from a ''zero strain'' intercalation mechanism in combination with a high potential of lithiation. LTO is considered ''zero strain'' because the phase change caused by lithiation/delithiation only results in a slight (0.2%) change in volume [201–203]. Electrochemically, this manifests itself as a small voltage hysteresis in its charge–discharge profile (Fig. 6d). In addition, a high equilibrium potential (~1.55 V vs. Li/Li$^+$) allows LTO to be operated in a potential window above 1 V, largely avoiding the formation and growth of the anode SEI, which can slow Li insertion and induce Li losses in graphite anodes (Table 3). Even when an SEI is formed, the lack of volume change enhances the SEI's stability. Since SEI impedance is not an issue, LTO nanoparticles can be used, similar to intercalation cathode material, which lead to higher rate performance at the expense of lower volumetric capacity [225,226]. In addition, LTO is extremely safe because its high potential prevents Li dendrite formation, even at high rates. Thus, although LTO does not have particularly high Li diffusivity or electrical conductivity, it is a good material for lower energy, but high power high cycle life Li-ion batteries.

Unfortunately, surface reactions are not completely avoidable with LTO anodes. LTO suffers from severe gassing due to a reaction between the organic electrolyte and the LTO active material [227]. This reaction can be suppressed by carbon coating, but carbon can also catalyze and accelerate electrolyte decomposition in the formation of an SEI, especially at high temperatures [228,229]. Even so, LTO anodes can last for tens of thousands of cycles giving

this electrode a distinct advantage over most other anode materials for high power applications [230,231].

Conversion materials – alloying materials (Type B)

Here, 'alloying materials' refer to elements which electrochemically alloy and form compound phases with Li (i.e. Type B conversion materials as in Eq. (2)) at a low potential (preferably below 1 V). Alloying materials can have extremely high volumetric and gravimetric capacity, but are notorious for their colossal volume change, expanding to several times the original volume upon lithiation (Fig. 6c illustrates how this occurs for Si). This can cause particles to fracture and lose electrical contact [232]. For anodes, volume change can destroy the SEI protective layer, resulting in continuous electrolyte decomposition, loss of Li inventory and increasing cell impedance. Alloying anodes thus generally suffer from short cycle life due to the loss of active material [233] and increasing cell impedance [234], especially at high mass loadings.

In general, the most successful strategy has been to produce a carbon composite in which the particles of alloying material have sufficiently small dimensions for mechanical stability, electron transport, and Li transport, while maintaining Li diffusion paths within the electrode (which commonly requires a hierarchical structure such as Fig. 2b [235]). To stabilize the SEI, the active material can be encapsulated in a carbon shell with a sufficient void space to allow for volume expansion (Fig. 2e) [236–241]. This may, in principle, stabilize the SEI and prevent particles from sintering into larger particles, enabling high cycle life even at high mass loadings [23]. Electrolyte additives can further stabilize the SEI and prolong the cycle life [242–244], and binders which bond to the active material, have high stiffness and swell minimally in electrolytes can provide additional mechanical stability if a carbon shell is not used [245–249]. Even so, high mass loading electrodes with high (>800 mAh cm^{-3}) volumetric capacity and long cycle life (10^3+ cycles) in full Li-ion battery cells have yet to be demonstrated. Also, nanoparticles inherently have high surface area, which result in large quantities of SEI formation and large irreversible capacity loss during the initial cycles.

Of all alloying materials, Si has received the most attention due to its relatively low average delithiation potential, extremely high gravimetric and volumetric capacity, abundance, lost cost, chemical stability, and non-toxicity. Sn has also been of high interest, having similar properties except with lower gravimetric capacity, slightly lower cell voltage, but higher electrical conductivity. However, Sn appears to suffer from easy fracturing (Fig. 2a), even when the particle dimensions are decreased to the 10 nm range [250]. Ge does not fracture even at larger particles sizes [251,252], but is too expensive for most practical application (Fig. 1a). Ga also has an interesting property of being liquid near room temperature [253], but is again too expensive.

Of the cost effective Li alloying metals, Zn, Cd, and Pb have good volumetric capacity, but suffer from low gravimetric capacity. Al also suffers from severe fracturing even with nano dimensions, as confirmed by in situ transmission electron microscopy (TEM) [254]. P and Sb have received some attention in recent years. Both elements have good capacity, and well performing electrodes have been constructed by merely ball milling the material with carbon [255,256]. However, both elements are toxic, have relatively high delithiation potentials, and Sb is additionally not very

abundant (Fig. 1). Phosphorus is also particularly dangerous due to its potential to form phosphine.

Conversion materials – other (Type A)

In the past, one popular approach to developing conversion materials was to use oxides in which Li_2O are formed on the initial charging of the battery. The Li_2O acts as a 'glue' to keep particles of the alloying material (such as Si or Sn) together [257], while also reducing the overall volume change within particles. However, Li_2O has low electrical conductivity, and this approach inevitably results in a large irreversible capacity and a large voltage hysteresis, much of which remains even at extremely slow rates [258]. Alternatively, the Li_2O itself can be used as an active material if the voltage range is significantly widened, enabling the use of non-alloying transition metals (such as Manganese(II)Oxide, Fig. 6d). This reduces the first cycle capacity loss and increases the charge capacity, but has the obvious issue of further reducing the potential difference with the cathode. Also, if the Li_2O phase is consumed, the nanoparticles of active alloying materials can sinter into larger particles and increase resistance [259,260]. Furthermore, the process generally also results in large volume change, causing issues similar to alloying anodes.

Of the various Type A conversion anode materials, MgH_2 and $Li_{1.07}V_{0.93}O_2$ are interesting in that they both have relatively small voltage hysteresis and delithiation potentials, although at low rates [261,262]. However, no studies have shown that these electrodes are viable at higher rates, and the demonstrated cycle life is short as well. Similarly, some phosphide and nitride electrodes have been shown to have relatively low voltage hysteresis, but only at low charge/discharge rates for several cycles [186].

Conclusion

The Li-ion battery has clear fundamental advantages and decades of research which have developed it into the high energy density, high cycle life, high efficiency battery that it is today. Yet research continues on new electrode materials to push the boundaries of cost, energy density, power density, cycle life, and safety. Various promising anode and cathode materials exist, but many suffer from limited electrical conductivity, slow Li transport, dissolution or other unfavorable interactions with electrolyte, low thermal stability, high volume expansion, and mechanical brittleness. Various methods have been pursued to overcome these challenges, as summarized in Fig. 3. Many intercalation cathodes have been brought to market, and conversion material technology is slowly coming closer to a widespread commercialization. The last couple of decades have been an exciting time for research in the field of Li-ion battery electrode materials. As new materials and strategies are found, Li-ion batteries will no doubt have an ever greater impact on our lives in the years to come.

Acknowledgements

References

[1] J.M. Tarascon, M. Armand, Nature 414 (6861) (2001) 359.
[2] S. Pacala, R. Socolow, Science 305 (5686) (2004) 968.
[3] H. Vikström, et al. Appl. Energy 110 (2013) 252.
[4] P.W. Gruber, et al. J. Ind. Ecol. 15 (5) (2011) 760.
[5] J. Speirs, et al. Renew. Sustain. Energy Rev. 35 (2014) 183.
[6] C. Grosjean, et al. Renew. Sustain. Energy Rev. 16 (3) (2012) 1735.
[7] M. Lowe, et al., Lithium-ion Batteries for Electric Vehicles: The U.S. Value Chain, Center on Globalization, Governance & Competitiveness, 2010.
[8] P.A. Nelson, et al., Modeling the Performance and Cost of Lithium-Ion Batteries for Electric-Drive Vehicles, Argonne National Laboratory, 2012.
[9] N.N. Greenwood, A. Earnshaw, Chemistry of the Elements, 2nd ed., Butterworth-Heinemann, Burlington, MA, 1997.
[10] InfoMine, Mining Intelligence and Technology, 2014.
[11] MetalPrices.com (2014).
[12] Metal Bulletin, Global Metal News, Metal Prices & Analysis, 2014.
[13] USGS, Minerals Information, 1932–2013.
[14] S. Moores, How is Natural Graphite Priced? Industrial Minerals, 2013.
[15] Sulfur Price, National Iranian Gas Company, 2014.
[16] G. Zhou, et al. Energy Environ. Sci. 7 (4) (2014) 1307.
[17] H. Gwon, et al. Energy Environ. Sci. 7 (2) (2014) 538.
[18] Y. Hu, X. Sun, J. Mater. Chem. A (2014).
[19] X. Wang, et al. Adv. Mater. 26 (28) (2014) 4763.
[20] K. Xie, B. Wei, Adv. Mater. 26 (22) (2014) 3592.
[21] J.-M. Tarascon, Philos. Trans. R. Soc. A: Math. Phys. Eng. Sci. 368 (1923) (2010) 3227.
[22] W.J. Lee, et al. Chem. Commun. 50 (52) (2014) 6818.
[23] N. Liu, et al. Nat. Nano 9 (3) (2014) 187.
[24] D.W. Murphy, F.A. Trumbore, J. Electrochem. Soc. 123 (7) (1976) 960.
[25] M.S. Whittingham, Science 192 (4244) (1976) 1126.
[26] M.S. Whittingham, Chem. Rev. 104 (10) (2004) 4271.
[27] M.S. Islam, C.A. Fisher, Chem. Soc. Rev. 43 (1) (2014) 185.
[28] J. Cho, et al. Chem. Mater. 12 (12) (2000) 3788.
[29] M. Yoncheva, et al. J. Mater. Sci. 46 (22) (2011) 7082.
[30] A. Sobkowiak, et al. Chem. Mater. 25 (15) (2013) 3020.
[31] J. Tu, et al. Electrochim. Acta 51 (28) (2006) 6456.
[32] F. Lin, et al. Nat. Commun. (2014) 5.
[33] S.K. Martha, et al. J. Electrochem. Soc. 158 (10) (2011) A1115.
[34] A. Jain, et al. APL Mater. 1 (1) (2013) 011002.
[35] G. Che, et al. J. Electrochem. Soc. 144 (12) (1997) 4296.
[36] J. Cho, et al. Angew. Chem. Int. Ed. 42 (14) (2003) 1618.
[37] T. Ohzuku, et al. J. Electrochem. Soc. 140 (7) (1993) 1862.
[38] P. Bruce, et al. J. Mater. Chem. 9 (1) (1999) 193.
[39] R. Wang, et al. Adv. Energy Mater. 3 (10) (2013) 1358.
[40] M.-J. Lee, et al. Nano Lett. (2014).
[41] S. Choi, A. Manthiram, J. Electrochem. Soc. 149 (2) (2002) A162.
[42] A. Yamada, et al. J. Electrochem. Soc. 148 (3) (2001) A224.
[43] D. Choi, et al. Nano Lett. 10 (8) (2010) 2799.
[44] J. Lloris, et al. Electrochem. Solid State Lett. 5 (10) (2002) A234.
[45] J. Barker, et al. J. Power Sources 146 (1–2) (2005) 516.
[46] K. Mizushima, et al. Mater. Res. Bull. 15 (6) (1980) 783.
[47] R. Yazami, et al. New Trends in Intercalation Compounds for Energy Storage and Conversion: Proceedings of the International Symposium, The Electrochemical Society, vol. 2003, 2003, p. 317.
[48] A. Du Pasquier, et al. J. Power Sources 115 (1) (2003) 171.
[49] J.R. Dahn, et al. Solid State Ionics 69 (3–4) (1994) 265.
[50] N. Williard, et al. Energies 6 (9) (2013) 4682.
[51] D. Doughty, E.P. Rother, Electrochem. Soc. Interface 21 (2) (2012) 35.
[52] J.N. Reimers, J. Dahn, J. Electrochem. Soc. 139 (8) (1992) 2091.
[53] G. Ceder, et al. Nature 392 (6677) (1998) 694.
[54] R. Alcántara, et al. J. Power Sources 81–82 (1999) 547.
[55] S. Madhavi, et al. Electrochim. Acta 48 (3) (2002) 219.
[56] R. Stoyanova, et al. Solid State Ionics 73 (3–4) (1994) 233.
[57] J. Cho, et al. Angew. Chem. 113 (18) (2001) 3471.
[58] I.D. Scott, et al. Nano Lett. 11 (2) (2010) 414.
[59] A. Rougier, et al. J. Electrochem. Soc. 143 (4) (1996) 1168.
[60] H. Arai, et al. Solid State Ionics 109 (3) (1998) 295.

[61]　P. Kalyani, N. Kalaiselvi, Sci. Technol. Adv. Mater. 6 (6) (2005) 689.
[62]　S.L. Dalton, et al., Lithium metal oxide materials and methods of synthesis and use, Google Patents (2008).
[63]　C. Chen, et al. J. Power Sources 128 (2) (2004) 278.
[64]　I. Bloom, et al. J. Power Sources 124 (2) (2003) 538.
[65]　Y. Itou, Y. Ukyo, J. Power Sources 146 (1) (2005) 39.
[66]　A.R. Armstrong, P.G. Bruce, Nature 381 (6582) (1996) 499.
[67]　M. Gu, et al. ACS Nano 7 (1) (2012) 760.
[68]　M. Wohlfahrt-Mehrens, et al. J. Power Sources 127 (1–2) (2004) 58.
[69]　S.R. Gowda, et al. Phys. Chem. Chem. Phys. 16 (15) (2014) 6898.
[70]　H. Zheng, et al. J. Power Sources 207 (2012) 134.
[71]　D.P. Abraham, et al. Electrochem. Solid State Lett. 11 (12) (2008) A226.
[72]　X. Han, et al. J. Power Sources 251 (2014) 38.
[73]　Y.I. Jang, et al. Electrochem. Solid State Lett. 1 (1) (1998) 13.
[74]　G. Ceder, S. Mishra, Electrochem. Solid State Lett. 2 (11) (1999) 550.
[75]　E. Rossen, et al. Solid State Ionics 57 (3–4) (1992) 311.
[76]　K. Kang, et al. Science 311 (5763) (2006) 977.
[77]　N. Yabuuchi, T. Ohzuku, J. Power Sources 119–121 (2003) 171.
[78]　K.M. Shaju, P.G. Bruce, Adv. Mater. 18 (17) (2006) 2330.
[79]　M.M. Thackeray, et al. J. Mater. Chem. 17 (30) (2007) 3112.
[80]　S. Hy, et al. J. Am. Chem. Soc. 136 (3) (2013) 999.
[81]　Y.-K. Sun, et al. Nat. Mater. 8 (4) (2009) 320.
[82]　M.M. Thackeray, Prog. Solid State Chem. 25 (1) (1997) 1.
[83]　M.M. Thackeray, et al. J. Power Sources 21 (1) (1987) 1.
[84]　M.M. Thackeray, J. Am. Ceram. Soc. 82 (12) (1999) 3347.
[85]　D.K. Kim, et al. Nano Lett. 8 (11) (2008) 3948.
[86]　F. Jiao, P.G. Bruce, Adv. Mater. 19 (5) (2007) 657.
[87]　E. Hosono, et al. Nano Lett. 9 (3) (2009) 1045.
[88]　H.-W. Lee, et al. Nano Lett. 10 (10) (2010) 3852.
[89]　Y.L. Ding, et al. Adv. Funct. Mater. 21 (2) (2011) 348.
[90]　Y.-K. Sun, et al. Electrochim. Acta 48 (5) (2003) 503.
[91]　T. Kakuda, et al. J. Power Sources 167 (2) (2007) 499.
[92]　B. Deng, et al. Electrochim. Acta 49 (11) (2004) 1823.
[93]　T. Numata, et al. J. Power Sources 97–98 (2001) 358.
[94]　Z. Chen, K. Amine, J. Electrochem. Soc. 153 (2) (2006) A316.
[95]　B. Li, et al. J. Mater. Chem. A 1 (41) (2013) 12954.
[96]　F. Jiao, et al. Angew. Chem. 120 (50) (2008) 9857.
[97]　K.S. Nanjundaswamy, et al. Solid State Ionics 92 (1–2) (1996) 1.
[98]　M. Armand, et al., Method for synthesis of carbon-coated redox materials with controlled size, Google Patents US (2004).
[99]　S.-Y. Chung, et al. Nat. Mater. 1 (2) (2002) 123.
[100]　C. Delacourt, et al. Electrochem. Solid State Lett. 9 (7) (2006) A352.
[101]　Y.J. Lee, et al. Science 324 (5930) (2009) 1051.
[102]　S.-i. Nishimura, et al. Nat. Mater. 7 (9) (2008) 707.
[103]　J. Kim, et al. Energy Environ. Sci. 6 (3) (2013) 830.
[104]　C. Delacourt, et al. J. Electrochem. Soc. 152 (5) (2005) A913.
[105]　S. Okada, et al. J. Power Sources 97 (2001) 430.
[106]　J. Wolfenstine, J. Allen, J. Power Sources 136 (1) (2004) 150.
[107]　H. Gwon, et al. Adv. Funct. Mater. 19 (20) (2009) 3285.
[108]　H. Huang, et al. Adv. Mater. 14 (21) (2002) 1525.
[109]　N. Recham, et al. Nat. Mater. 9 (1) (2010) 68.
[110]　T. Mueller, et al. Chem. Mater. 23 (17) (2011) 3854.
[111]　J. Barker, et al. J. Electrochem. Soc. 150 (10) (2003) A1394.
[112]　C. Masquelier, L. Croguennec, Chem. Rev. 113 (8) (2013) 6552.
[113]　B. Sergio, P. Stefania, Nanotechnology for Sustainable Energy, vol. 1140, American Chemical Society, (2013), p. 67.
[114]　F. Wang, et al. Nat. Commun. 3 (2012) 1201.
[115]　F. Wang, et al. J. Am. Chem. Soc. 133 (46) (2011) 18828.
[116]　A.J. Gmitter, et al. J. Power Sources 217 (2012) 21.
[117]　F. Badway, et al. Chem. Mater. 19 (17) (2007) 4129.
[118]　F. Wu, et al. Adv. Energy Mater. 4 (11) (2014).
[119]　M.Q. Zhao, et al. Nat. Commun. 5 (2014) 3410.
[120]　C. Luo, et al. ACS Nano 7 (9) (2013) 8003.
[121]　D.-W. Wang, et al. J. Mater. Chem. A 1 (33) (2013) 9382.
[122]　Y.L. Wang, et al. Energy Environ. Sci. 4 (10) (2011) 3947.
[123]　T. Li, et al. Electrochim. Acta 68 (2012) 202.
[124]　C. Li, et al. Adv. Energy Mater. 3 (1) (2013) 113.
[125]　Z. Zhang, et al. RSC Adv. 4 (30) (2014) 15489.
[126]　F. Badway, et al. J. Electrochem. Soc. 150 (10) (2003) A1318.
[127]　Y. Zheng, et al. Solid State Commun. 152 (17) (2012) 1703.
[128]　H.C. Yu, et al. Energy Environ. Sci. 7 (5) (2014) 1760.
[129]　A.J. Gmitter, et al. J. Mater. Chem. 20 (20) (2010) 4149.
[130]　X. Hua, et al. J. Phys. Chem. C (2014).

[131]　P. Liu, et al. J. Phys. Chem. C 116 (10) (2012) 6467.
[132]　M.A. Reddy, et al. Adv. Energy Mater. 3 (3) (2013) 308.
[133]　R. Ma, et al. J. Mater. Chem. A 1 (47) (2013) 15060.
[134]　L. Li, et al. Nano Lett. 12 (11) (2012) 6030.
[135]　Z.-W. Fu, et al. J. Electrochem. Soc. 152 (2) (2005) E50.
[136]　Y.-H. Cui, et al. Electrochim. Acta 56 (5) (2011) 2328.
[137]　D.H. Lee, et al. Electrochim. Acta 59 (2012) 213.
[138]　D.H. Lee, et al. Phys. Chem. Chem. Phys. 16 (7) (2014) 3095.
[139]　J.-l. Liu, et al. Electrochem. Commun. 13 (3) (2011) 269.
[140]　L. Xiao, et al. Adv. Mater. 24 (9) (2012) 1176.
[141]　J. Zheng, et al. Nano Lett. 14 (5) (2014) 2345.
[142]　Y. Yang, et al. J. Am. Chem. Soc. 134 (37) (2012) 15387.
[143]　K. Cai, et al. Nano Lett. 12 (12) (2012) 6474.
[144]　F. Wu, et al. Adv. Energy Mater. (2014).
[145]　F. Wu, et al. Part. Part. Syst. Charact. 31 (6) (2014) 639.
[146]　H.-J. Peng, et al. Adv. Funct. Mater. 24 (19) (2014) 2772.
[147]　C. Nan, et al. J. Am. Chem. Soc. 136 (12) (2014) 4659.
[148]　A. Abouimrane, et al. J. Am. Chem. Soc. 134 (10) (2012) 4505.
[149]　D. Kundu, et al. J. Power Sources 236 (2013) 112.
[150]　L. Liu, et al. RSC Adv. 4 (18) (2014) 9086.
[151]　L. Liu, et al. Chem. Commun. 49 (98) (2013) 11515.
[152]　C. Luo, et al. Adv. Funct. Mater. 24 (26) (2014) 4082.
[153]　Y. Liu, et al. J. Mater. Chem. A (2014).
[154]　Z. Wei-Jun, J. Power Sources (2011) 196.
[155]　D.R. Lide, Handbook of Chemistry and Physics, CRC Press, Boca Raton, FL, 2005
[156]　S.W. Kim, et al. Adv. Mater. 22 (46) (2010) 5260.
[157]　R. Ma, et al. Nanoscale 5 (14) (2013) 6338.
[158]　Q. Chu, et al. Electrochim. Acta 111 (2013) 80.
[159]　X. He, et al. J. Power Sources 190 (1) (2009) 154.
[160]　M. Ebner, et al. Science 342 (6159) (2013) 716.
[161]　W. Li, et al. Proc. Natl. Acad. Sci. U. S. A. 110 (18) (2013) 7148.
[162]　N. Jayaprakash, et al. Angew. Chem. 50 (26) (2011) 5904.
[163]　Z. Wei Seh, et al. Nat. Commun. 4 (2013) 1331.
[164]　Z.W. Seh, et al. Chem. Sci. 4 (9) (2013) 3673.
[165]　Z.W. Seh, et al. Chem. Sci. (2013).
[166]　Z.W. Seh, et al. Energy Environ. Sci. (2013).
[167]　M. Nagao, et al. J. Mater. Chem. 22 (19) (2012) 10015.
[168]　Y. Fu, et al. J. Am. Chem. Soc. 135 (48) (2013) 18044.
[169]　K.P. Cai, et al. Nano Lett. 12 (12) (2012) 6474.
[170]　G. Luo, et al. J. Renew. Sustain. Energy 4 (6) (2012) 063128.
[171]　F. Wu, et al. J. Mater. Chem. A 2 (17) (2014) 6064.
[172]　D. Aurbach, et al. J. Electrochem. Soc. 156 (8) (2009) A694.
[173]　Z. Lin, et al. Adv. Funct. Mater. 23 (8) (2013) 1064.
[174]　E. Peled, et al. J. Power Sources 26 (3–4) (1989) 269.
[175]　L. Suo, et al. Nat. Commun. 4 (2013) 1481.
[176]　J.T. Lee, et al. Adv. Mater. 25 (33) (2013) 4573.
[177]　J. Hassoun, B. Scrosati, Adv. Mater. 22 (45) (2010) 5198.
[178]　Z. Lin, et al. Angew. Chem. 125 (29) (2013) 7608.
[179]　Z. Lin, et al. ACS Nano 7 (3) (2013) 2829.
[180]　C.-P. Yang, et al. Angew. Chem. Int. Ed. 52 (32) (2013) 8363.
[181]　W. Xu, et al. Energy Environ. Sci. 7 (2) (2014) 513.
[182]　N.A. Kaskhedikar, J. Maier, Adv. Mater. 21 (25–26) (2009) 2664.
[183]　G.-N. Zhu, et al. Energy Environ. Sci. 5 (5) (2012) 6652.
[184]　Z. Chen, et al. Adv. Funct. Mater. 23 (8) (2013) 959.
[185]　N. Nitta, G. Yushin, Part. Part. Syst. Charact. 31 (3) (2014) 317.
[186]　J. Cabana, et al. Adv. Mater. 22 (35) (2010) E170.
[187]　C.-M. Park, et al. Chem. Soc. Rev. 39 (8) (2010) 3115.
[188]　Y. Yamada, et al. ACS Appl. Mater. Interfaces (2014).
[189]　K. Teshima, et al. Cryst. Growth Des. 11 (10) (2011) 4401.
[190]　M.K.Y. Chan, et al. J. Am. Chem. Soc. 134 (35) (2012) 14362.
[191]　T.D. Hatchard, J.R. Dahn, J. Electrochem. Soc. 151 (6) (2004) A838.
[192]　K. Zhong, et al. J. Power Sources 196 (16) (2011) 6802.
[193]　M.E. Spahr, in: M. Yoshio, et al. (Eds.), Lithium-Ion Batteries: Science and Technologies, Springer, 2009, pp. 117.
[194]　M.D. Levi, D. Aurbach, J. Phys. Chem. B 101 (23) (1997) 4641.
[195]　E. Markevich, et al. J. Electroanal. Chem. 580 (2) (2005) 231.
[196]　K. Persson, et al. J. Phys. Chem. Lett. 1 (8) (2010) 1176.
[197]　D. Billaud, et al. Mater. Res. Bull. 14 (7) (1979) 857.
[198]　Y. Qi, et al. J. Electrochem. Soc. 157 (5) (2010) A558.
[199]　N. Takami, et al. J. Electrochem. Soc. 158 (6) (2011) A725.
[200]　F. Wunde, et al. J. Power Sources 215 (2012) 109.
[201]　S. Scharner, et al. J. Electrochem. Soc. 146 (3) (1999) 857.
[202]　M. Wagemaker, et al. Adv. Mater. 18 (23) (2006) 3169.

[203] J.-F. Colin, et al. Electrochem. Commun. 12 (6) (2010) 804.
[204] R. Chandrasekaran, et al. J. Electrochem. Soc. 157 (10) (2010) A1139.
[205] N. Ding, et al. Solid State Ionics 180 (2–3) (2009) 222.
[206] J. Xie, et al. Mater. Chem. Phys. 120 (2–3) (2010) 421.
[207] J.C. Li, et al. J. Phys. Chem. C 116 (1) (2012) 1472.
[208] M. Pharr, et al. Nano Lett. 12 (9) (2012) 5039.
[209] S.P. Ong, et al. Comput. Mater. Sci. 68 (2013) 314.
[210] A. Chockla, et al. ACS Appl. Mater. Interfaces 4 (9) (2012) 4658.
[211] B. Laforge, et al. J. Electrochem. Soc. 155 (2) (2008) A181.
[212] L. Baggetto, P.H.L. Notten, J. Electrochem. Soc. 156 (3) (2009) A169.
[213] I.A. Courtney, et al. Phys. Rev. B 58 (23) (1998) 15583.
[214] J. Xie, et al. Solid State Ionics 181 (35–36) (2010) 1611.
[215] J.L. Tirado, Mater. Sci. Eng. R: Rep. 40 (3) (2003) 103.
[216] J.Y. Huang, et al. Science 330 (6010) (2010) 1515.
[217] D. Aurbach, et al. Electrochim. Acta 45 (1–2) (1999) 67.
[218] D. Bar-Tow, et al. J. Electrochem. Soc. 146 (3) (1999) 824.
[219] H. Nozaki, et al. J. Power Sources 194 (1) (2009) 486.
[220] Carbon Powders for Lithium Battery Systems, Timcal Graphite & Carbon, Switzerland, 2005.
[221] M. Winter, et al. Adv. Mater. 10 (10) (1998) 725.
[222] R. Mukherjee, et al. Nat. Commun. (2014) 5.
[223] J.R. Dahn, et al. Science 270 (5236) (1995) 590.
[224] T. Zheng, et al. J. Electrochem. Soc. 142 (8) (1995) 2581.
[225] H.-G. Jung, et al. Nat. Commun. 2 (2011) 516.
[226] F.X. Wu, et al. Electrochim. Acta 78 (2012) 331.
[227] Y.-B. He, et al. Sci. Rep. (2012) 2.
[228] Y.-B. He, et al. J. Power Sources 239 (2013) 269.
[229] M.-S. Song, et al. J. Mater. Chem. A 2 (3) (2014) 631.
[230] K. Zaghib, et al. J. Power Sources 196 (8) (2011) 3949.
[231] SCiB: Super Charge Ion battery, Toshiba.
[232] J. Wang, et al. Angew. Chem. Int. Ed. 53 (17) (2014) 4460.
[233] C.K. Chan, et al. Nat. Nano 3 (1) (2008) 31.
[234] Y. Oumellal, et al. J. Mater. Chem. 21 (17) (2011) 6201.
[235] A. Magasinski, et al. Nat. Mater. 9 (4) (2010) 353.
[236] B. Hertzberg, et al. J. Am. Chem. Soc. 132 (25) (2010) 8548.
[237] B. Wang, et al. Adv. Mater. 25 (26) (2013) 3560.
[238] N. Liu, et al. Nano Lett. 12 (6) (2012) 3315.
[239] S. Chen, et al. Phys. Chem. Chem. Phys. 14 (37) (2012) 12741.
[240] Y. Park, et al. Adv. Energy Mater. 3 (2) (2013) 206.
[241] H. Tao, et al. Nanoscale 6 (6) (2014) 3138.
[242] H. Nakai, et al. J. Electrochem. Soc. 158 (7) (2011) A798.
[243] S. Dalavi, et al. J. Electrochem. Soc. 159 (5) (2012) A642.
[244] A. Bordes, et al. J. Power Sources 257 (2014) 163.
[245] J. Li, et al. Electrochem. Solid State Lett. 10 (2) (2007) A17.
[246] N.S. Hochgatterer, et al. Electrochem. Solid State Lett. 11 (5) (2008) A76.
[247] A. Magasinski, et al. ACS Appl. Mater. Interfaces 2 (11) (2010) 3004.
[248] I. Kovalenko, et al. Science 333 (6052) (2011) 75.
[249] M.-H. Ryou, et al. Adv. Mater. 25 (11) (2013) 1571.
[250] L. Xu, et al. Nano Lett. (2013).
[251] X.H. Liu, et al. Nano Lett. 11 (9) (2011) 3991.
[252] W. Liang, et al. ACS Nano (2013).
[253] H. Okamoto, J. Phase, Equilib. Diffus. 27 (2) (2006) 200.
[254] Y. Liu, et al. Nano Lett. 11 (10) (2011) 4188.
[255] J. Qian, et al. Chem. Commun. 48 (71) (2012) 8931.
[256] A. Darwiche, et al. J. Am. Chem. Soc. 134 (51) (2012) 20805.
[257] I.A. Courtney, J.R. Dahn, J. Electrochem. Soc. 144 (6) (1997) 2045.
[258] M.V. Reddy, et al. Chem. Rev. (2013).
[259] I.A. Courtney, J.R. Dahn, J. Electrochem. Soc. 144 (9) (1997) 2943.
[260] L.Q. Zhang, et al. Micron 43 (11) (2012) 1127.
[261] Y. Oumellal, et al. Nat. Mater. 7 (11) (2008) 916.
[262] A.R. Armstrong, et al. Nat. Mater. 10 (3) (2011) 223.